Closed-Form Takeoff Weight Estimation Model for Air Transportation Simulation

Hak-Tae Lee* and Gano B. Chatterji†

University of California Santa Cruz, Moffett Field, CA, 94035, USA

Takeoff weight is an important parameter for computing accurate aircraft trajectories. Most systems used for simulating air traffic and for providing air traffic management decision support use takeoff weights that depend only on the aircraft type. This paper proposes a closed-form algorithm for estimating takeoff weights based on flight plan and aircraft performance data. The algorithm is derived by combining the constant-altitude-cruise range equation with the weight estimation procedure commonly used in aircraft design. The model first determines whether the payload is limited by payload capacity, maximum takeoff weight, or fuel tank capacity, and then calculates the takeoff weight accordingly. The model is verified against manufacturer provided payload range diagrams for a jet and a turboprop aircraft. Accurate and fast takeoff weight estimation with negligible computational overhead will enhance large scale air traffic simulations by improving the accuracy of trajectories and fuel burn estimates. Improvement in trajectory and fuel burn estimates will benefit the assessment of noise and emissions as well as improve the accuracy of automated conflict detection and resolution algorithms.

Nomenclature

S	= reference wing area, [m^2]
c	= thrust specific fuel consumption (TSFC), [1/s]
C_{D0}	= parasitic drag coefficient
C_{D2}	= induced drag coefficient
V	= cruise speed, [m/s]
V_g	= groundspeed, [m/s]
V_w	= wind speed, [m/s]
d	= wind-compensated distance, [m]
d_g	= flight route distance, [m]
d_{alt}	= distance to alternate airport, [m]
d_{hold}	= distance for holding, [m]
h	= cruise altitude, [m]
q	= dynamic pressure, [N/m^2]
t_{hold}	= extra holding time, [s]
f_{inc}	= climb fuel increment factor
f_{man}	= maneuver fuel factor
f_{res}	= reserve fuel factor
W_F	= fuel weight, [N]
W_{Fs}	= fuel weight for segment s, [N]
$(W_F)_A^B$	= required fuel weight to cruise from A to B, [N]
W_{MF}	= maximum fuel weight, [N]
W_i	= aircraft weight at the beginning of cruise, [N]
W_f	= aircraft weight at the end of cruise, [N]
W_{TO}	= takeoff weight, [N]
W_{MTO}	= maximum takeoff weight, [N]

*Associate Scientist, U. C. Santa Cruz, M/S 210-8, AIAA Member.

†Scientist, U. C. Santa Cruz, M/S 210-8, AIAA Associate Fellow.

W_E = empty weight, [N]
W_{ZF} = zero fuel weight, [N]
W_{MZF} = maximum zero fuel weight, [N]
W_{PLD} = payload weight, [N]
W_{MPLD} = maximum payload weight, [N]

Symbols

ψ_g = ground track heading, [rad]
ψ_w = wind heading, [rad]

I. Introduction

TAKEOFF weight is an important aircraft performance parameter that affects climb and descent gradients, as well as total fuel burn. For air transportation simulations, accurate climb and descent gradients are essential for conflict detection and resolution.[1] Accurate takeoff weight estimation is also crucial for assessing economic and environmental impacts,[2] because the total fuel burn is a function of the takeoff weight, and the noise signature is sensitive to the climb and descent gradient.

Weight estimation has been researched for different applications. Cavcar and Cavcar[3] constructed an approximate model for constant altitude transonic cruise. Their work is focused on aiding aircraft design. Williams and Green[4] described the weight estimation model in NASA's Center-Terminal Area Approach Control Automation System. In this system, weight at the beginning of descent is estimated by subtracting the fuel burn rate multiplied by the flight time from the takeoff weight. If those data are not available, the system uses a pre-specified typical descent weight for each aircraft type. In commercial operations, fuel weight is calculated as a part of flight planning. Flight planning systems employ higher fidelity models that involve iterative processes, and those models are often proprietary.[5]

In this study, a simple yet accurate takeoff weight estimation model for jet and turboprop aircraft that is suitable for large scale air transportation simulations is developed. As these simulations generally need to process tens of thousands of flights, a closed-form solution method is developed by combining the constant-altitude-cruise range equation with a weight estimation technique from aircraft design.[6] It is difficult to derive an analytical expression that accurately estimates the weight of the climb fuel, because the standard climb procedure that maintains a calibrated airspeed schedule produces complicated variations in the true airspeed and climb rate. This study handles the climb segment by adapting a climb fuel increment factor from aircraft design and by creating a least square curve fit for this factor. Consequently, the model maintains accuracy even when the cruise segment is relatively short.

Aircraft performance data come from the Base of Aircraft Data,[7] and operational parameters such as route distance, cruise speed, and cruise altitude come from the filed flight plan. The model consists of a set of algebraic equations that first determines whether the payload is limited by maximum payload capacity, maximum takeoff weight, or fuel tank capacity. Once this phase of payload limitation is determined, maximum allowable payload is computed for the given conditions, and the fuel weight, including reserve fuel weight, is calculated.

The rest of the paper is organized as follows. Section II describes each flight segment. In Section III, the approximate model for estimating the climb fuel is explained in detail. In Section IV, a derivation process of the closed-form solution is presented. Section V compares payload range diagrams created using the weight estimation method with real world data for verification. Section VI compares trajectory simulation results and shows the effect of takeoff weight. Finally, Section VII concludes the paper.

II. Fuel Weight for Each Flight Segment

For the takeoff weight computation, three basic flight segments (climb, cruise, and descent) are examined. The characteristics of each segment, as well as the appropriate model for estimating the fuel consumption for the given segment, are investigated. The weight of additional fuel required for maneuvers and reserve are also discussed.

A. Climb Segment

An aircraft maintains a specified calibrated airspeed (CAS) schedule that is a function of altitude during climb. Engine thrust is set to the maximum climb thrust. Using the total energy equation, climb rate is determined by true airspeed (TAS) and thrust. Since the TAS and thrust continuously vary as the aircraft climbs, it is not trivial to analytically integrate the fuel consumption during the climb segment.

A technique used in aircraft design is to apply a climb fuel increment factor.[6] This factor, f_{inc}, is defined as the additional fuel required to climb, W_{Finc}, compared to the amount of fuel that is required to cruise the same distance at the cruise altitude divided by the takeoff weight, W_{TO}, as described in Eq. (1). This relation is illustrated in Fig. 1.

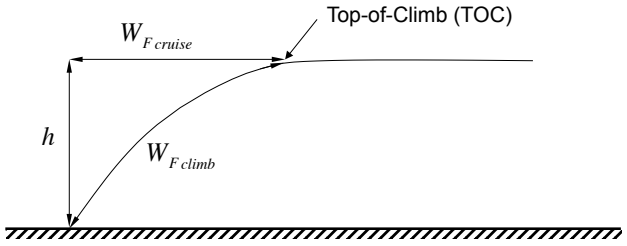

Figure 1. Climb fuel and corresponding cruise fuel.

$$f_{inc} = \frac{W_{Finc}}{W_{TO}} = \frac{W_{Fclimb} - (W_{Fcruise})_{departure}^{TOC}}{W_{TO}} \tag{1}$$

Two dominant parameters for computing f_{inc} are cruise altitude, h, and cruise speed, V, as shown in Eq. (2). Equation (2) was developed based on the fuel burn data from a DC-9-30, a DC-8-62, and a DC-10-10.[6] For the current study, a more elaborate approximation that captures the characteristics of each aircraft type is developed using the trajectory simulations based on BADA. Details of this approximation are discussed in Section III.

$$f_{inc} = \frac{h\,[ft]}{316} + \left(\frac{V\,[knot]}{84.4}\right)^2 \tag{2}$$

B. Cruise Segment

The commonly used range equation, Breguet's range equation,[8] was derived assuming a constant lift to drag ratio. If an aircraft is assumed to maintain its maximum lift to drag ratio, Breguet's equation is expressed as in Eq. (3). W_i is the initial weight at the beginning of the cruise segment and W_f is the final weight at the end of the cruise segment. c is the thrust specific fuel consumption that is a characteristic of each aircraft. For jets and turboprops, c is a function of TAS. C_{D0} and C_{D2} are parasitic and induced drag coefficients at cruise condition. To maintain its lift to drag ratio at maximum value, an aircraft has to climb slowly.

$$d = \frac{V}{c}\frac{1}{2\sqrt{C_{D0}C_{D2}}}\left(\ln W_i - \ln W_f\right) \tag{3}$$

However, in actual operations, most aircraft maintain a preferred cruise altitude. Instead of the Breguet's range equation, the constant-altitude-cruise range equation described in Hale[9] is required. This equation, shown in Eq. (4), is rearranged to use the parameters given in the BADA. The dynamic pressure, q, is a function of h and V. S is the reference wing area of the aircraft. Equation (4) forms the basis of computing the takeoff weight.

$$d = \frac{V}{c}\frac{1}{\sqrt{C_{D0}C_{D2}}}\left(\tan^{-1}\left(\frac{W_i}{qS}\sqrt{\frac{C_{D2}}{C_{D0}}}\right) - \tan^{-1}\left(\frac{W_f}{qS}\sqrt{\frac{C_{D2}}{C_{D0}}}\right)\right) \tag{4}$$

If the wind forecast along the route is available, wind-compensated distance, d, can be used instead of flight route distance, d_g. When there is wind, groundspeed is not identical to airspeed. Figure 2 shows the relation between airspeed, wind speed, and groundspeed. groundspeed[10] can be computed using Eq. (5). d is computed using Eq. (6). Flying the given ground track distance with wind is equivalent to flying the wind-compensated distance without wind.

$$V_g = V\cos\left(\sin^{-1}\left(\frac{V_w}{V}\sin\left(\psi_w - \psi_g\right)\right)\right) + V_w\cos\left(\psi_w - \psi_g\right) \tag{5}$$

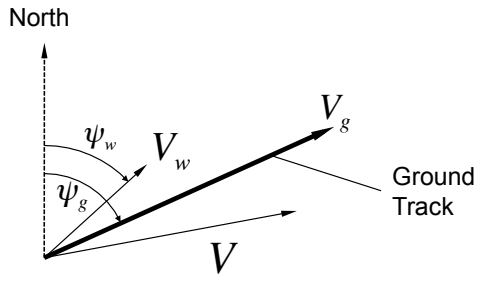

Figure 2. If wind forecast is available, groundspeed can be computed to account for the effect of wind.

$$d = \frac{V}{V_g} d_g \tag{6}$$

C. Descent Segment

Fuel consumption in descent is significantly lower than that in climb or cruise. However, the fuel used during descent is small compared to the total fuel consumption, so it is replaced by the fuel required to cruise the same distance as from the top-of-descent (TOD) to the landing airport.[6] The substitution will slightly overestimate the amount of required fuel, but it can be considered an extra safety factor on top of the reserve fuel.

$$W_{F\,descent} \simeq (W_{F\,cruise})_{TOD}^{arrival} \tag{7}$$

D. Maneuver and Reserve Fuel

The fuel required for warm-up, taxi, takeoff, approach, landing, and other possible maneuvers is consolidated into a single item called maneuver fuel. The maneuver fuel weight, $W_{F\,man}$, is generally expressed as a fixed percentage of W_{TO} as shown in Eq. (8). The typical value of f_{man} is around 0.007.[6]

$$W_{F\,man} \simeq f_{man} W_{TO} \tag{8}$$

The Federal Aviation Administration (FAA) specifies requirements for minimum reserve fuel. Reserve fuel for international operations must be enough to support climb from sea level to cruise altitude, cruise to an alternate airport at best speed and altitude, descent to sea level, and cruise for 45 minutes at cruise speed and altitude. The reserve fuel is generally expressed as a fixed percentage of the zero-fuel weight, W_{ZF}, as shown in Eq. (9). W_{ZF} is the sum of empty weight, W_E, and payload, W_{PLD}, which is the weight of an aircraft with payload but without fuel. The typical value of f_{res} is around 0.08.[6] For domestic operations, FAA regulation requires reserve fuel only for cruising to an alternate airport and for 45 minutes of holding. In this case, the two requirements can be handled by extending the cruise distance instead of using Eq. (9)

$$W_{F\,res} \simeq f_{res} W_{ZF} \tag{9}$$

III. Approximated Model for Climb Fuel Consumption

Among the three basic flight segments, the amount of fuel consumed during climb is the most difficult to estimate. In this section, a method based on fitting the trajectory simulation results is presented in detail. Previously discussed Eq. (2) is based on energy conservation that does not accurately capture the energy lost from aerodynamic drag during climb. Moreover, Eq. (2) is derived from a narrow family of aircraft and might not be suitable for other types of aircraft. The new method creates a quadratic function of h and V for each aircraft type to reflect its unique climb performance characteristics.

A quadratic function of h and V as shown in Eq. (10) is chosen to represent f_{inc} as an expansion to Eq. (2). Additional terms, h^2, hV, V, and a constant are added to capture effects that are not directly represented by a simple

conservation of potential and kinetic energy. These effects include changing atmospheric condition as a function of h, variations in TAS, and the dependency of the thrust specific fuel consumption on TAS.

$$f_{inc}(h,V) = \frac{W_{Fclimb} - (W_{Fcruise})_{departure}^{TOC}}{W_{TO}} = k_1 h^2 + k_2 hV + k_3 V^2 + k_4 h + k_5 V + k_6 \tag{10}$$

Actual climb fuel is computed by a simulation that follows the procedures specified in BADA.[7] Since the simulation provides a complete trajectory, the horizontal distance to the top-of-climb (TOC) and the weight at the TOC can be extracted for given h and V. Actual climb fuel weight, W_{Fclimb}, is the difference between W_{TO} and the weight at TOC. Cruise fuel weight, $(W_{Fcruise})_{departure}^{TOC}$, is calculated by setting d in Eq. (4) as the horizontal distance between the departure airport and the TOC.

The coefficients, k_js, are computed by applying a least square fit to data points generated by running the trajectory simulations with ranges of W_{TO}, h, and V.

Three W_{TO}s, 60%, 80%, and 100% of the maximum takeoff weight, W_{MTO}, are used. f_{inc} is not fully independent of the takeoff weight; however, the dependency is fairly weak. One of the purposes of this approximation is to generate a fit that is not a function of W_{TO}. This weak dependency plays a key role in deriving simple equations for the takeoff weight, which will be described later.

h is varied from 10,000 ft to 45,000 ft with 1,000 ft steps for jet aircraft and from 10,000 ft to 35,000 ft for turboprop aircraft. V is varied from 300 knots to 500 knots with 10 knot steps for jets and from 200 knots to 350 knots for turboprops. A total of 2,268 combinations of W_{TO}, h, and V were simulated for each aircraft type in the jet category, and 1,248 combinations were simulated for each aircraft type in the turboprop category.

Not all of the combinations are feasible. For each aircraft type, the trajectory simulation results are filtered to exclude unreachable regions of the flight envelope. Using feasible data points, an initial least square fit is created. This fit describes the behavior of f_{inc} well except for the combinations of h and V that are not likely to be used, such as high h with low V or low h with high V. To prevent these unrealistic operation points from skewing the fit, another screening step is performed by filtering the data points that yield errors higher than $\pm 15\%$ from the initial fit. Final values of the coefficients are obtained by applying another least square fit to the screened data points.

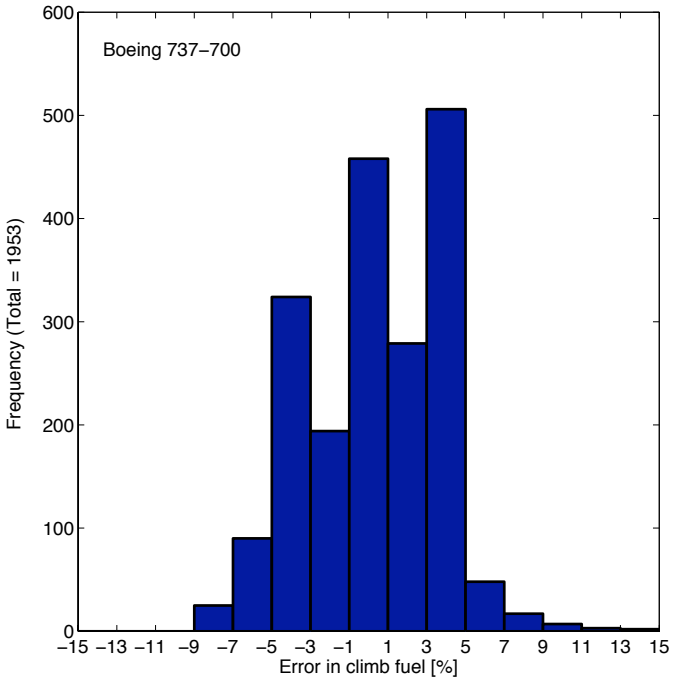

Figure 3. Distribution of error in climb fuel weight of Boeing 737-700.

The coefficients are computed for 17 widely used transport jet aircraft listed in Table 1 and four turboprop aircraft listed in Table 2. A total of 21 aircraft listed in Tables 1 and 2 represent 56% of flights among 47,735,790 flights that

were flown between 2005 and 2007.[2]

Figure 3 shows a histogram of errors in climb fuel weight for Boeing 737-700, which compares the climb fuel weights computed by the least square fit to those computed from the trajectory simulations. The error distribution shows three noticeable peaks caused by three different W_{TO}s used for the trajectory simulations. However, the errors are mostly within ± 5 %.

Table 1. List of coefficients for f_{inc} for common jet aircraft.

Aircraft	$k_1 \times 10^{12}$	$k_2 \times 10^{9}$	$k_3 \times 10^{9}$	$k_4 \times 10^{6}$	$k_5 \times 10^{6}$	$k_6 \times 10^{3}$
Dassault Falcon 50	-18.2	3.11	-163	2.46	47.1	-0.823
Embraer 145	17.3	4.72	-286	0.0268	77.5	-1.36
Canadair CRJ-100	9.74	1.11	133	1.07	-70.4	8.14
Airbus 319-100	20.7	-1.07	107	1.10	-46.3	5.91
Airbus 320-200	29.4	-2.63	64.2	1.40	-22.5	3.74
Airbus 330-200	30.6	-2.85	70.0	1.31	-21.5	3.29
Boeing 717-200	-31.4	4.62	-238	0.552	68.6	-3.34
Boeing 737-200	-42.7	5.64	-310	0.929	91.2	-4.61
Boeing 737-300	-23.7	3.96	-248	0.680	75.5	-4.53
Boeing 737-700	38.9	-3.37	130	1.48	-43.6	5.81
Boeing 737-800	31.1	-2.75	115	1.47	-40.3	5.12
Boeing 747-400	8.45	-0.816	44.4	1.03	-15.7	1.60
Boeing 757-200	-20.2	4.28	-264	0.447	78.4	-5.40
Boeing 767-300	-35.6	5.67	-279	0.180	86.3	-5.04
Boeing 777-200	21.9	-2.84	65.0	1.38	-17.1	2.56
Boeing MD82	-58.9	8.29	-364	0.290	106	-5.48
Boeing MD83	-30.0	4.55	-289	0.802	87.5	-5.64

Table 2. List of coefficients for f_{inc} for common large turboprop aircraft.

Aircraft	$k_1 \times 10^{12}$	$k_2 \times 10^{9}$	$k_3 \times 10^{9}$	$k_4 \times 10^{6}$	$k_5 \times 10^{6}$	$k_6 \times 10^{3}$
British Aerospace Jetstream 31	38.4	-15.2	-612	2.46	1.61	-10.6
Saab 340	-59.8	7.70	-374	1.98	58.7	-2.98
Embraer 120	25.7	-1.40	-353	1.01	82.5	-4.55
ATR 42-500	29.7	-6.41	-244	1.41	63.7	-3.96

IV. Computation of the Takeoff Weight

In this section, all the previously developed model equations for climb, cruise, and descent, as well as for maneuvers and reserve, are combined to derive the equations for calculating the takeoff weight. Since an aircraft has limits on takeoff weight, payload weight, and fuel capacity, the model will consist of a set of algebraic equations.

The total fuel weight, W_F, is the sum of the fuel weight for each segment and the additional fuel weights for maneuvers and reserve as shown in Eq. (11).

$$W_F = W_{F climb} + (W_{F cruise})_{TOC}^{TOD} + W_{F descent} + W_{F man} + W_{F res} \tag{11}$$

In Eq. (11), $W_{F climb}$ is substituted by Eq. (1); $W_{F descent}$ is approximated by cruise fuel as in Eq. (7); $W_{F man}$ and $W_{F res}$ are substituted using Eqs. (8) and (9) respectively. When all of these substitutions are combined, Eq. (11) is rearranged into Eq. (12).

$$
\begin{aligned}
W_F &= (W_{F\,cruise})_{departure}^{TOC} + (W_{F\,cruise})_{TOC}^{TOD} + (W_{F\,cruise})_{TOD}^{arrival} + \\
&\quad W_{TO} f_{inc} + f_{man} W_{TO} + f_{res} W_{ZF} \\
&= (W_{F\,cruise})_{departure}^{arrival} + (f_{inc} + f_{man})\, W_{TO} + f_{res} W_{ZF}
\end{aligned}
\tag{12}
$$

The first term of the right hand side of Eq. (12) is the fuel consumed while flying at constant speed and altitude for a given distance. This distance along the route of flight is, depending on the availability of wind forecast, the sum of flight route distances or wind-compensated distances between adjacent waypoints from the departure airport to the arrival airport as shown in Fig. 4. To account for the reserve fuel, the distance to an alternate arrival airport, d_{alt}, and the distance for a given duration of holding, d_{hold}, can be added to the route distance. For generality, reserve fuel as a fixed percentage of W_{ZF} will remain in the formulation. If d_{alt} and d_{hold} are used, f_{res} should be set to zero. The cruise fuel weight can be expressed as a function of distance and initial weight, which is W_{TO}, using Eq. (4) as shown in Eq. (13).

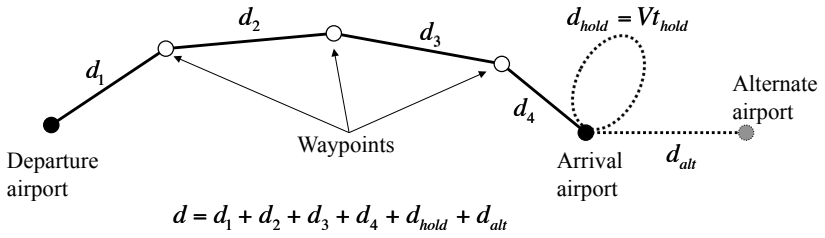

Figure 4. Distance is calculated by adding all the segment distances between the waypoints as well as the distance from the arrival airport to the alternate arrival airport.

$$
W_{F\,cruise} = W_{TO} - \frac{1}{A_1} \frac{A_1 W_{TO} - A_d}{1 + A_1 A_d W_{TO}} \tag{13}
$$

The auxiliary parameters, A_1, A_2, and A_d, in Eq. (13) are defined in Eqs. (14) through (16).

$$
A_1 = \frac{1}{qS} \sqrt{\frac{C_{D2}}{C_{D0}}} \tag{14}
$$

$$
A_2 = \frac{c}{V} \sqrt{C_{D2} C_{D0}} \tag{15}
$$

$$
A_d = \tan\left(A_2 d\right) \tag{16}
$$

Since W_F is W_{TO} subtracted by W_{ZF}, substituting $W_{F\,cruise}$ in Eq. (12) by Eq. (13) yields a quadratic equation of W_{TO} as shown in Eq. (17). The auxiliary parameters, A_3 and A_4, in Eq. (17) are defined in Eqs. (18) and (19). It is shown in Eq. (17) that f_{inc} being independent of W_{TO} enabled this quadratic formulation.

$$
\left(A_1 A_3 A_d\right) {W_{TO}}^2 + \left(A_1 A_4 A_d W_{ZF} + A_3 - 1\right) W_{TO} + \left(A_4 W_{ZF} + \frac{A_d}{A_1}\right) = 0 \tag{17}
$$

$$
A_3 = f_{inc} + f_{man} \tag{18}
$$

$$
A_4 = 1 + f_{res} \tag{19}
$$

W_{TO} can be obtained by solving Eq. (17), which has closed-form solutions. However, it is necessary to check the W_{ZF} corresponding to W_{MTO} to ensure W_{TO} does not exceed W_{MTO}. Eq. (17) can be solved for W_{ZF} as a function of W_{TO}, and the maximum zero-fuel weight, W_{MZF}, should be calculated from W_{MTO} as shown in Eq. (20).

$$W_{MZF} = \frac{-A_1 A_3 A_d {W_{MTO}}^2 + (1 - A_3) W_{MTO} - \frac{A_d}{A_1}}{A_4 (A_1 A_d W_{MTO} + 1)} \tag{20}$$

BADA provides W_E, maximum payload, W_{MPLD}, and W_{MTO}. If the sum of W_E and W_{MPLD} exceeds W_{MZF}, some of its payload has to be traded with the fuel weight. In this case, the W_{MTO} becomes W_{TO}.

Conversely, if the sum of W_E and W_{MPLD} is smaller than W_{MZF}, the aircraft can carry its maximum payload, and W_{TO} will be smaller than or equal to W_{MTO}. Since the load factor is not known, aircraft are assumed to carry as much payload as possible. W_{ZF} becomes the sum of W_E and W_{MPLD}, and W_{TO} is obtained by solving Eq. (17). Since Eq. (17) is a quadratic equation, two solutions are possible. A number of computations with realistic scenario revealed that the smaller of the two is the physically feasible solution.

Even though it is not provided by BADA, fuel tank capacity can often be obtained from various sources such as airport planning manuals. For very long cruise ranges, usually the fuel tank is full at its maximum fuel weight, W_{MF}, and the payload has to be reduced to be able to meet the given range. In this case, W_{TO} in Eq. (17) can be substituted by the sum of W_E, W_{PLD}, and W_{MF}, and rearranged for W_{PLD} as shown in Eq. (21).

$$B_2 {W_{PLD}}^2 + B_1 W_{PLD} + B_0 = 0 \tag{21}$$

The auxiliary parameters, B_0, B_1, and B_2, in Eq. (21) are defined in Eqs. (22) through (24).

$$\begin{aligned} B_0 \quad = \quad & A_1 A_d (A_3 + A_4) {W_E}^2 + A_1 A_d (2A_3 + A_4) W_E W_{MF} + A_1 A_3 A_d {W_{MF}}^2 + \\ & (A_3 + A_4 - 1) W_E + (A_3 - 1) W_{MF} + \tfrac{A_d}{A_1} \end{aligned} \tag{22}$$

$$B_1 = 2A_1 A_d (A_3 + A_4) W_E + A_1 A_d (2A_3 + A_4) W_{MF} + A_3 + A_4 - 1 \tag{23}$$

$$B_2 = A_1 A_d (A_3 + A_4) \tag{24}$$

Figure 5 summarizes the takeoff weight computation process. First step is calculating W_{MZF} that corresponds to W_{MTO} using Eq. (20) as shown in Fig. 5 (a). If sum of W_E and W_{MPLD} is smaller than W_{MZF} as in Fig. 5 (b), W_{MPLD} becomes the payload, and sum of W_E and W_{MPLD} becomes W_{ZF}. W_{TO} is determined by solving Eq. (17) as indicated in Fig. 5 (d). If sum of W_E and W_{MPLD} is larger than W_{MZF}, W_F is calculated by subtracting W_{MZF} from W_{MTO} as shown in Fig. 5 (c). If W_F is smaller than W_{MF} as described in Fig. 5 (e), the payload is limited by W_{MTO}. In this region, W_{TO} is always W_{MTO} as shown in Fig. 5 (f). If the calculated W_F in Fig. 5 (c) is larger than W_{MF}, W_F is fixed to W_{MF}, and W_{PLD} has to be reduced. W_{PLD} is calculated by Eq. (21), and W_{TO} is sum of W_E, W_{PLD}, and W_{MF} as indicated in Fig. 5 (g).

V. Verification of the Model

To verify the the model, payload range trade-off diagrams were created for a Boeing 737-200 as an example of a jet aircraft and for an Embraer E120 as an example of a turboprop aircraft. These aircraft were chosen because the data are available from both BADA and the manufacturers.

A. Payload Range Trade-off for Boeing 737-200

Unlike the payload range diagrams of more recent aircraft such as Boeing 737-700, the manufacturer-provided payload range data for Boeing 737-200 uses constant altitude cruise at 30,000 ft.[11] A long range cruise Mach number of 0.74 is used for the cruise Mach number, which is a typical value for the older generation Boeing 737 family of aircraft. Table 3 lists the complete set of parameters. Since the Boeing document did not specify detailed reserve fuel condition other than domestic reserve, three different conditions were tested.

Figure 6 shows the payload range diagrams. Payload is plotted with respect to range. The curve starts horizontal. This horizontal portion indicates that, if the required range is small, the aircraft can carry its maximum payload. In this region, payload is limited by the maximum payload capacity. The first downward slope after the horizontal part is the operating region which is limited by the maximum takeoff weight. In this region, the payload has to be traded for fuel to meet the required range, but the fuel tank is still not full. Finally, the second, steeper downward sloping

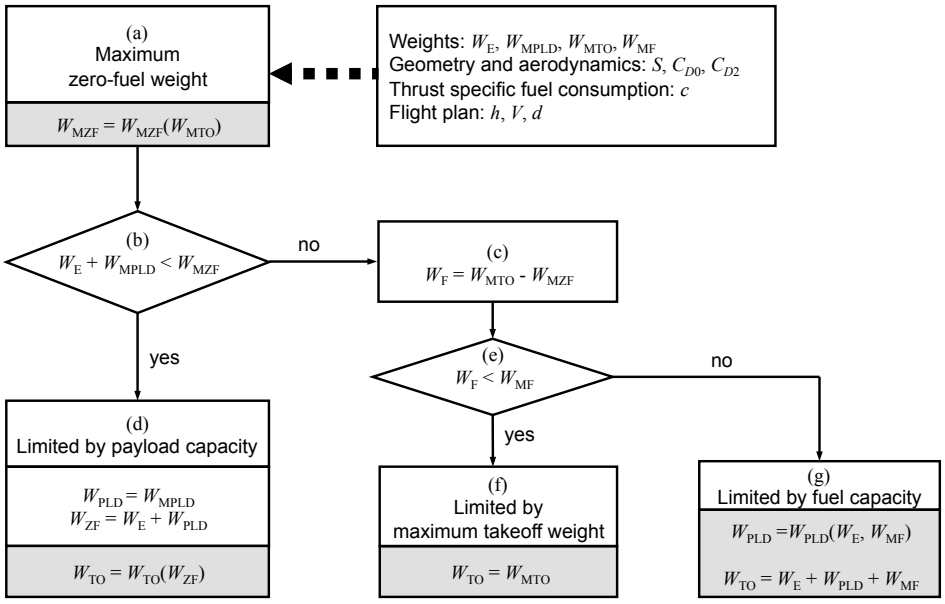

Figure 5. Summary flow chart of the takeoff weight computation process.

Table 3. List of parameters used for the payload range trade-off diagram of Boeing 737-200.

Aircraft type	Boeing 737-200 with JT9D-9/9A engines
h	9,144 m (30,000 ft)
Cruise Mach number	0.74
Atmospheric condition	Standard atmosphere, no wind
W_{MTO}	513,422 N (115,500 lbs)
W_E	265,825 N (59,800 lbs)
W_{MPLD}	156,476 N (35,200 lbs)
W_{MF}	142,365 N (32,026 lbs)
f_{man}	0.007
Reserve fuel condition 1	$f_{res} = 0$, 45 min holding
Reserve fuel condition 2	$f_{res} = 0$, 100 nmi to alternate airport, 45 min holding
Reserve fuel condition 3	$f_{res} = 0.08$
C_{D0}	0.0214
C_{D2}	0.0462
S	91.09 m^2
c	2.131×10^{-4} 1/s

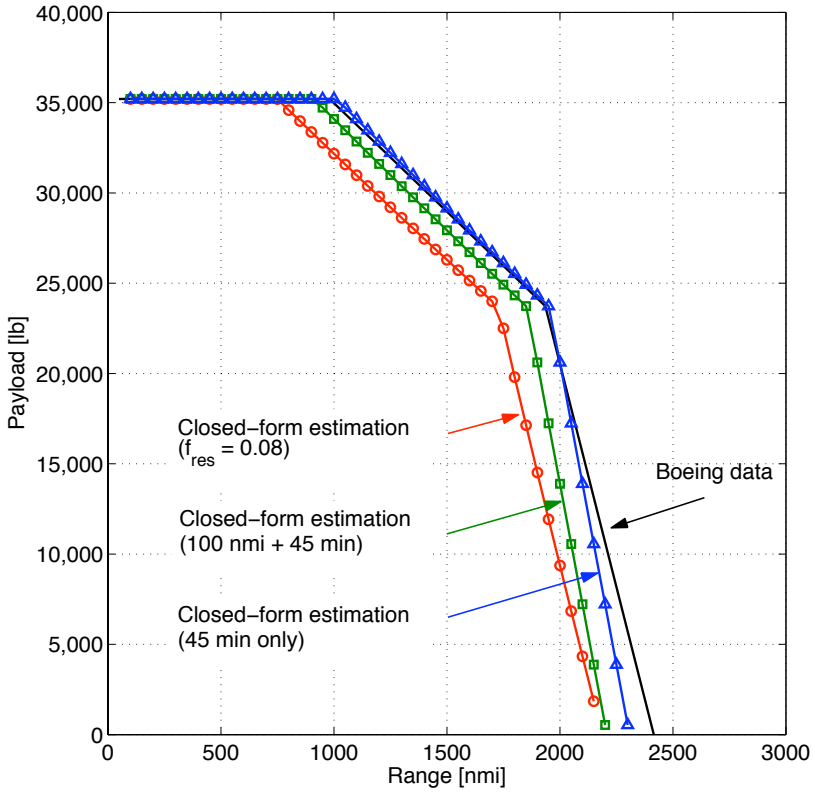

Figure 6. Payload range diagram for Boeing 737-200.

region indicates that the fuel tank is full. In this region, payload has to be further reduced to meet the required range, since it is not possible to add more fuel. The theoretical maximum range is achieved with a fully filled fuel tank and zero payload. As can be seen from the figure, resulting payload range relations from the model show the same general trends as with the manufacture's data. For the most conservative reserve fuel condition, the range is off by about 250 nautical miles for given payload. However this reserve condition is more suitable for international operations as discussed in the earlier section. Two other domestic reserve conditions show less than 100 nautical mile range differences, especially when the range is smaller than 2,000 nautical miles.

B. Payload Range Trade-off for Embraer 120

For the Embraer 120 RT, 315 knots was used for the maximum cruise speed.[12] Table 4 lists all of the parameters used for the computation. For this aircraft, the specific reserve condition, which is 100 nautical miles to the alternate airport with 45 minutes of holding, was provided. Figure 7 shows the payload range trade-off relation for Embraer 120. The curve from the model follows the manufacturer data within 50 nautical miles.

Table 4. List of parameters used for the payload range trade-off diagram of Embraer E120.

Aircraft type	Embraer E120 RT with PW118 engines
h	7,620 m (25,000 ft)
V	162 m/s (315 knots)
Atmospheric condition	Standard atmosphere, no wind
W_{MTO}	112,700 N (25,353 lbs)
W_E	70,854 N (15,939 lbs)
W_{MPLD}	32,046 N (7,209 lbs)
W_{MF}	25,480 N (5,732 lbs)
f_{man}	0.007
Reserve fuel condition	$f_{res} = 0$, 100 nmi to alternate airport, 45 min holding
C_{D0}	0.025
C_{D2}	0.05
S	39.43 m^2
c	1.366×10^{-4} 1/s

VI. Trajectory Comparison

Takeoff weights, fuel consumption, and climb gradients for five Boeing 737-300 flights extracted from Southwest Airline's schedule were computed to show the impact of takeoff weight on total fuel burn and climb gradients. In Table 5, the first three columns are actual flight plan information. No wind is assumed for the weather condition. For reserve fuel condition, $f_{res} = 0.08$ is used instead of d_{alt} and d_{hold}.

Two sets of trajectories were simulated. In the first set, all five fights were initialized with the maximum takeoff weight of 138,450 lbs. In the second set, flights were initialized with the weights calculated using the weight estimation model that is developed in this paper. These weights are shown in the fourth column of the table. First two sub-columns under the Fuel burn column compare the total fuel burn. Weights under the label "at W_{MTO}" are the fuel burn computed by the trajectory simulations when the flights were initialized with maximum takeoff weight. Weights under the label "at W_{TO}" are the fuel burn for trajectory simulations when each flight was initialized with its estimated takeoff weight. The comparison shows that using the maximum takeoff weight overestimates the fuel burn by around five to ten percent. The first two sub-columns under Climb gradient column compare the average climb gradients for ground to TOC. Gradients under the label "at W_{MTO}" are for the trajectories that are initialized with the maximum takeoff weight. Gradients under the label "at W_{TO}" are for the trajectories that are initialized with estimated takeoff weights. Using maximum takeoff weight causes about 14 to 22 percent underestimation of the climb gradient.

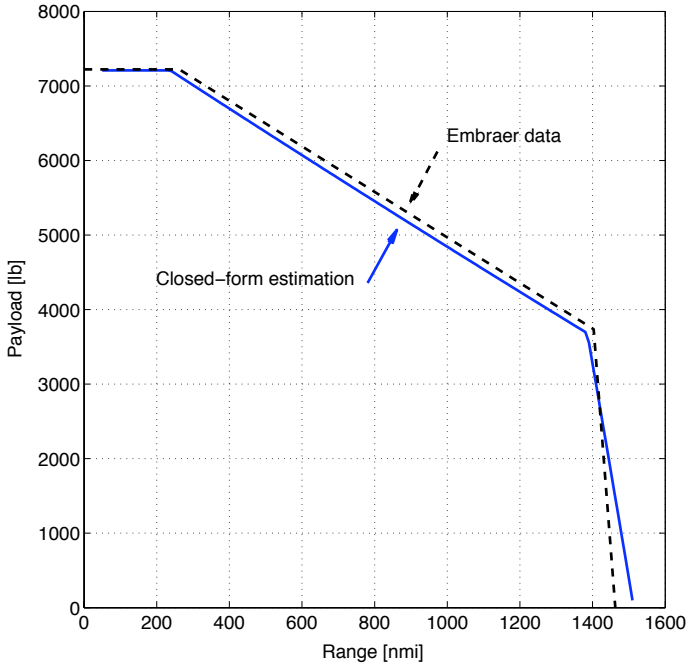

Figure 7. Payload range diagram for Embraer 120.

Table 5. Fuel burn and climb gradient comparison between Boeing 737-300 flights using maximum takeoff weight and the takeoff weights estimated with the method in this paper.

h	V	d	W_{TO}	Fuel burn [lb]			Climb gradient [deg]		
[ft]	[knot]	[nmi]	[lb]	at W_{MTO}	at W_{TO}	Diff. [%]	at W_{MTO}	at W_{TO}	Diff. [%]
23000	406	245	120,450	3,918	3,614	8.4	4.4	5.4	-19.1
33000	445	416	122,586	6,339	5,777	9.7	2.5	3.2	-22.3
22000	400	594	125,566	9,121	8,631	5.7	4.7	5.5	-13.9
33000	443	571	124,537	8,466	7,789	8.7	2.5	3.1	-19.8
33000	434	408	122,469	6,291	5,714	10.1	2.5	3.2	-22.4

VII. Conclusions

A non-iterative closed-form solution is developed for the takeoff weight estimation. Using this formulation, a takeoff weight that is based on aircraft performance and flight plan can be quickly calculated for a flight. The effect of cruise altitude and speed are accurately captured in addition to the required range. For verification, payload range trade-off diagrams are created and compared to that provided by the manufacturers. Comparison shows that the model captures all three phases of payload limitation with about 50 to 100 nautical mile differences in the range.

Accurate and fast takeoff weight estimation will benefit large scale air traffic simulations by providing more accurate trajectories. Especially, it will be useful for the evaluation of automated conflict detection and resolution schemes where trajectory prediction is crucial. As environmental impact of aviation is becoming increasingly important, this model can also improve the fidelity of system-wide noise and emission estimation.

While the upper bound of the takeoff weight is the maximum takeoff weight, the closed-form model provides the lower bound of the takeoff weight. Investigations with real world takeoff weight and trajectory data will further enhance the takeoff weight estimation model.

References

[1]Erzberger, H. and Paielli, R. A., "Concept for Next Generation Air Traffic Control System," *Air Traffic Control Quarterly*, Vol. 10, No. 4, Oct. 2002, pp. 355–378.

[2]Palopo, K., Windhorst, R. D., Suharwardy, S., and Lee, H.-T., "Wind-Optimal Routing in the National Airspace System," *9th AIAA Aviation Technology, Integration, and Operations Conference*, Hilton Head, SC, Sep. 21-23, 2009.

[3]Cavcar, A. and Cavcar, M., "Approximate solutions of range for constant altitude - constant high subsonic speed flight of transport aircraft," *Aerospace Science and Technology*, Vol. 8, No. 6, 2004, pp. 557–567.

[4]Williams, D. H. and Green, S. M., "Flight Evaluation of Center-TRACON Automation System Trajectory Prediction Process," NASA TP 1998-208439, NASA, Jul. 1998.

[5]Cooper, M. L. and Altus, S. S., "Aircraft Flight Plan Optimization for Minimizing Emissions," US Patent No. US 2009/0204453 A1, Aug. 2009.

[6]Kroo, I. M., *Aircraft Design: Sysnthesis and Analysis*, 1st ed., Desktop Aeronautics, Palo Alto, CA, Sep. 2006.

[7]EUROCONTROL, "User Manual for the Base of Aircraft Data (BADA) Revision 3.6," No. ACE-C-E2, Jul. 2004.

[8]Anderson, J. D., *Introduction to Flight*, 3rd ed., McGraw-Hill, Singapore, 1989.

[9]Hale, F. J., *Introduction to Aircraft Performance, Selection and Design*, John Wiley and Sons, Inc., New York, NY, 1984.

[10]Chatterji, G. B., Sridhar, B., and Bilimoria, K. D., "En-route Flight Trajectory Prediction for Conflict Avoidance and Traffic Management," *AIAA, Guidance, Navigation and Control Conference*, San Diego, CA, Jul. 29-31, 1996.

[11]Boeing Company, "737 Airplane Characteristics for Airport Planning," Boeing Commercial Airplanes, Oct. 2005.

[12]Embraer, "EMB120 Brasilia Airport Planning Manual," No. A.P.-120/731, Empresa Brasileira de Aeronautica S. A., Oct. 2000.